IJMMM International Journal of Minerals, Metallurgy and Materials 矿物冶金与材料学报（英文版）

Solid-state reaction of a $CaO–V_2O_5$ mixture: A fundamental study for the vanadium extraction process

Jun-yi Xiang, Xin Wang, Gui-shang Pei, Qing-yun Huang, and Xue-wei Lü

Cite this article as:
Jun-yi Xiang, Xin Wang, Gui-shang Pei, Qing-yun Huang, and Xue-wei Lü, Solid-state reaction of a $CaO–V_2O_5$ mixture: A fundamental study for the vanadium extraction process, *Int. J. Miner. Metall. Mater.*, 28(2021), No. 9, pp. 1462-1468. https://doi.org/10.1007/s12613-020-2136-7

Articles you may be interested in

Jing Wen, Tao Jiang, Mi Zhou, Hui-yang Gao, Jia-yi Liu, and Xiang-xin Xue, Roasting and leaching behaviors of vanadium and chromium in calcification roasting–acid leaching of high-chromium vanadium slag, *Int. J. Miner. Metall. Mater.*, 25(2018), No. 5, pp. 515-526. https://doi.org/10.1007/s12613-018-1598-3

Jing-peng Wang, Yi-min Zhang, Jing Huang, and Tao Liu, Synergistic effect of microwave irradiation and CaF_2 on vanadium leaching, *Int. J. Miner. Metall. Mater.*, 24(2017), No. 2, pp. 156-163. https://doi.org/10.1007/s12613-017-1390-9

Dong Wang, Sheng Pang, Chun-yue Zhou, Yan Peng, Zhi Wang, and Xu-zhong Gong, Improve titanate reduction by electro-deoxidation of $Ca_3Ti_2O_7$ precursor in molten $CaCl_2$, *Int. J. Miner. Metall. Mater.*, 27(2020), No. 12, pp. 1618-1625. https://doi.org/10.1007/s12613-020-2165-2

Hendrik Setiawan, Himawan Tri Bayu Murti Petrus, and Indra Perdana, Reaction kinetics modeling for lithium and cobalt recovery from spent lithium-ion batteries using acetic acid, *Int. J. Miner. Metall. Mater.*, 26(2019), No. 1, pp. 98-107. https://doi.org/10.1007/s12613-019-1713-0

Song-tao Yang, Mi Zhou, Tao Jiang, and Xiang-xin Xue, Isothermal reduction kinetics and mineral phase of chromium-bearing vanadium-titanium sinter reduced with CO gas at 873-1273 K, *Int. J. Miner. Metall. Mater.*, 25(2018), No. 2, pp. 145-152. https://doi.org/10.1007/s12613-018-1557-z

Xiao-yi Shen, Hong-mei Shao, Ji-wen Ding, Yan Liu, Hui-min Gu, and Yu-chun Zhai, Zinc extraction from zinc oxidized ore using $(NH_4)_2SO_4$ roasting–leaching process, *Int. J. Miner. Metall. Mater.*, 27(2020), No. 11, pp. 1471-1481. https://doi.org/10.1007/s12613-020-2015-2

IJMMM WeChat

QQ author group

International Journal of Minerals, Metallurgy and Materials
Volume 28, Number 9, September 2021, Page 1462
https://doi.org/10.1007/s12613-020-2136-7

Solid-state reaction of a $CaO-V_2O_5$ mixture: A fundamental study for the vanadium extraction process

Jun-yi Xiang[1)], *Xin Wang*[1)], *Gui-shang Pei*[1)], *Qing-yun Huang*[2)], *and Xue-wei Lü*[1,3)]

1) College of Materials Science and Engineering, Chongqing University, Chongqing 400044, China
2) School of Metallurgy and Materials Engineering, Chongqing University of Science and Technology, Chongqing 401331, China
3) Chongqing Key Laboratory of Vanadium-Titanium Metallurgy and Advanced Materials, Chongqing University, Chongqing 400044, China
(Received: 28 April 2020; revised: 4 July 2020; accepted: 6 July 2020)

Abstract: The aim of this study was to investigate the phase transformation and kinetics of the solid-state reaction of $CaO-V_2O_5$, which is the predominant binary mixture involved in the vanadium recovery process. Thermal analysis, X-ray diffraction spectroscopy, scanning electron microscopy, and energy dispersive spectrometry were used to characterize the solid-state reaction of the samples. The extent of the solid reaction was derived using the preliminary quantitative phase analysis of the X-ray patterns. The results indicate that the solid reaction of the $CaO-V_2O_5$ mixture is strongly influenced by the reaction temperature and CaO/V_2O_5 mole ratio. The transformation of calcium vanadate involves a step-by-step reaction of $CaO-V_2O_5$, $CaO-CaV_2O_6$, and $CaO-Ca_2V_2O_7$ depending on the CaO/V_2O_5 mole ratio. The kinetic data of the solid reaction of the $CaO-V_2O_5$ (1:1) mixture followed a second-order reaction model. The activation energy (E_a) and preexponential factor (A) were determined to be 145.38 kJ/mol, and 3.67×10^8 min^{-1}, respectively.

Keywords: calcium vanadate; vanadium extraction; solid-state reaction; kinetics

1. Introduction

The calcification roasting–acid leaching process, as a clean production method for the extraction of vanadium from metallurgical slags, was first proposed by the Russia Tula factory in the 1970s [1]. This process involves the oxidation roasting of vanadium slag with lime or limestone at approximately 900°C in a multihearth furnace or rotary kiln to convert vanadium compounds to soluble calcium vanadate, followed by the extraction of vanadium from the roasted slag by leaching in dilute sulfuric acid or sodium hydroxide solution, and then the preliminary vanadium product is obtained from the leaching solution via precipitation, solvent extraction, or the ion exchange method [2–3]. Calcification roasting–acid leaching is an environmentally friendly process because it eliminates the use of corrosive gas, has a low additive (lime or limestone) cost, and generates less harmful wastewater and a small amount of noxious solid waste [4–5].

$CaO-V_2O_5$ is the predominant system for the roasting of vanadium slag with lime or limestone. The phase diagram and thermodynamic data of $CaO-V_2O_5$ have been reviewed in the literature [6]. The $CaO-V_2O_5$ system contains four intermediate compounds: metavanadate (CaV_2O_6), pyrovanadate ($Ca_2V_2O_7$), orthovanadate ($Ca_3V_2O_8$), and tetracalcium vanadate ($Ca_4V_2O_9$) [7]. Among these compounds, CaV_2O_6, $Ca_2V_2O_7$, and $Ca_3V_2O_8$ are vital for the vanadium extraction process [8–9]. The solubilities of CaV_2O_6, $Ca_2V_2O_7$, and $Ca_3V_2O_8$ in water at 25°C are 0.022, 0.0035, and 0.012 mol/L, respectively [10]; however, they have good solubilities in acidic or alkali solutions. Thus, the transformation of calcium vanadate is of vital importance for the extraction process [5].

Most vanadium is involved in phase with corundum $(Fe_{1-x}V_x)_2O_3$, the pyroxene $M_2Si_2O_6$ structure, or spinel $M^{2+}M^{3+}_2O_4$ (M^{2+} = Ni, Ca, Mg, Mn, or Fe; M^{3+} = Fe, V, Ti, Cr, or Al) [11]. The transformation of calcium vanadate is strongly influenced by roasting conditions such as the roasting temperature, holding time, atmosphere, additives, heating rate, and so on [12–14]. During roasting, normal vanadium spinel first converts to inverse vanadium spinel at a lower roasting temperature [15]. Then, vanadium spinel and its decomposition product, vanadium oxide, combine with CaO to generate CaV_2O_6 at low temperature and $Ca_2V_2O_7$ at approximately 630°C. $Ca_3V_2O_8$ can be generated with an excess amount of CaO above 750°C [10]. At a low CaO content in the slag, the system undergoes a CaO deficiency for

Corresponding authors: Jun-yi Xiang E-mail: xiangjunyi126@126.com; Xue-wei Lü E-mail: lvxuewei@163.com

complete fixation of V_2O_5 into calcium vanadate. At a high CaO content, vanadium partly dissolves in perovskite, which does not undergo structural changes upon roasting [16]. A lower heating rate was found to promote the conversion of vanadium and make the optimum roasting temperature shift to the high temperature region [1]. Furthermore, the calcification roasting process can be enhanced using microwave heating [17] and mechanical activation pretreatment [18] and by improving the oxygen partial pressure [9].

The formation of calcium vanadate is thermodynamically favorable [19]; however, the actual process is usually limited by the dynamic conditions [1]. Therefore, the kinetic data for the solid−solid reaction of a $CaO-V_2O_5$ mixture are very important for industrial applications. The present investigation was therefore undertaken to clarify the phase evolution of the $CaO-V_2O_5$ mixture at different temperatures. The conversion degree of the solid-state reaction of the $CaO-V_2O_5$ mixture was determined using X-ray quantitative phase analysis and the solid−solid reaction kinetics were examined.

2. Experimental

2.1. Materials

The CaO and V_2O_5 used in the experiments were of analytical grade with a purity greater than 99.9% and were preheated at 900 and 500°C, respectively, for 5 h to remove free water and crystal water. The samples were cooled to approximately 100°C in a furnace and further cooled to room temperature in a dryer with allochroic silica.

2.2. Experimental procedure

A determined amount of CaO and V_2O_5 with varied mole ratios was thoroughly ground and mixed in an agate mortar. The thermal analysis of the mixture was conducted on a simultaneous thermogravimetry and differential scanning calorimetry (TG−DSC; STA 449C, NETZSCH, Germany). Approximately 15 mg of the mixture was loaded in an alumina crucible and heated from 30 to 800°C at a constant rate of 2°C/min. Air (21vol% O_2 and 79vol% N_2) was flowed into the furnace at a rate of 50 mL/min during heating. Each experiment was performed twice for reproducibility and exact thermograms were obtained. The solid reaction experiments were performed in a muffle furnace and regulated to ±2°C via a temperature programmed control instrument. A determined amount of $CaO-V_2O_5$ mixture was roasted at a determined temperature for different times by placing the cold alumina crucible into a preheated muffle furnace and removing it while hot. In this way, the heating and cooling rates were kept approximately equal.

2.3. Analytical methods

The mineralogical composition of the samples was identified via X-ray powder diffraction (XRD) using an X-ray diffractometer (PANalytical X'Pert Powder, PANalytical B. V.) with Cu K_α radiation (λ = 0.154 nm, 40 kV, 75 mA) at room temperature. The 2θ scan range was from 10° to 60° at a rate of 0.01°/s. The phase analysis of the X-ray diffractograms was performed using the search/match software program MDI Jade 6.0 applied to the ICDD Powder Diffraction File database. The preliminary quantitative phase analyses were assessed using the Rietveld method [20]. This method creates an approximate model of the diffractogram based on input parameters. This model is then refined by the least squares method in iterative steps until the best possible approximation to the measured pattern is found. The scanning electron microscopy (SEM)/energy dispersive X-ray spectroscopy (EDS) analysis of the samples was performed using a scanning electron microscope (VEGA 3 LMH; TESCAN, Czech Republic) equipped with an energy dispersive X-ray spectroscope (Oxford, UK).

3. Results and discussion

3.1. TG−DSC analysis

The TG and DSC curves for the $CaO-V_2O_5$ (1:1, mole ratio, so as the follows) mixture are provided in Fig. 1, which shows that the weight loss up to 402°C is 4.47%, corresponding to the release of adsorbed water molecules in the mixture. The release of these water molecules produces the corresponding endothermic peak in the DSC curves over the same temperature ranges. A weight loss of 0.87% is observed in the range of 402–600°C, which should correspond to the volatilization of V_2O_5; however, the weight of the sample is almost constant at above 600°C. Two sharp endothermic peaks are detected at 623.4 and 769.7°C that can be attributed to the fusion of V_2O_5 and CaV_2O_6, respectively.

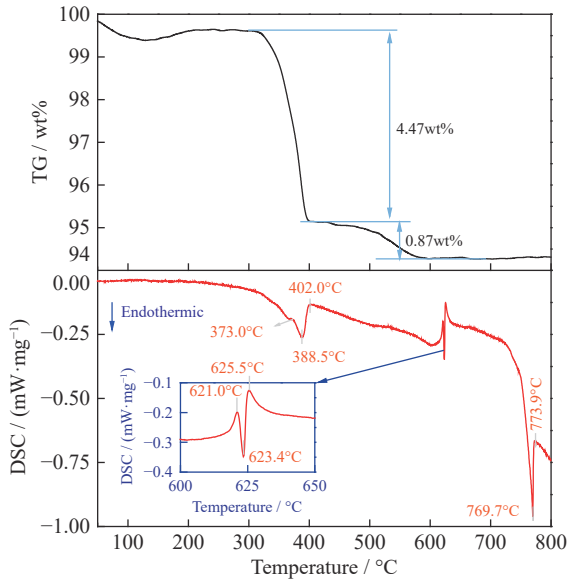

Fig. 1. TG-DSC analysis of the $CaO-V_2O_5$ (1:1) mixture.

These fusion data are consistent with the reported peaks at 630 and 770°C [21].

3.2. Phase transformation

Fig. 2 shows the XRD patterns of the products of the $CaO-V_2O_5$ (1:1) mixture roasted at 400, 450, 500, 550, and 600°C for 40 h. As seen in Fig. 2, three major phases are apparent from the XRD patterns, namely, CaO, V_2O_5, and CaV_2O_6. The intensity of V_2O_5 and CaO gradually decreased with the increase in temperature from 400 to 500°C and continued to decrease slightly from 500 to 600°C. In the meantime, the intensity of CaV_2O_6 gradually increased with an increase in temperature. No other intermediate compounds were found under these experimental conditions.

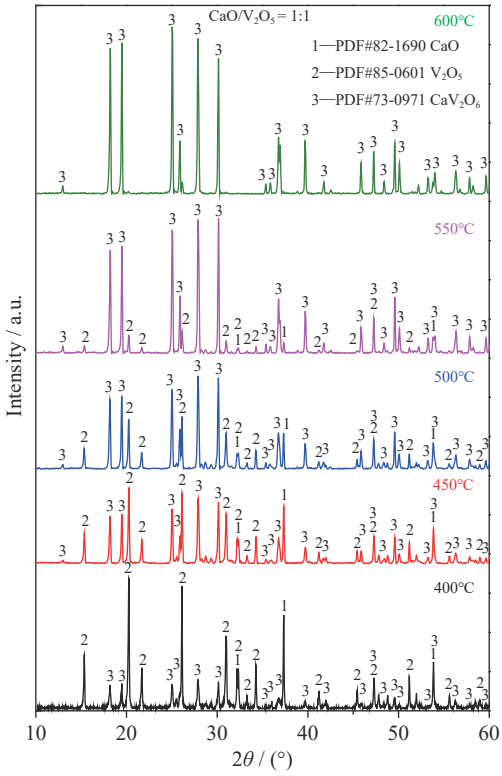

Fig. 2. XRD patterns of the products of the $CaO-V_2O_5$ (1:1) mixture roasted at different temperatures.

Fig. 3 shows the preliminary quantitative analysis results of the X-ray patterns of the $CaO-V_2O_5$ mixtures with different CaO/V_2O_5 mole ratios roasted at different temperatures. As shown in Fig. 3(a), for the $CaO-V_2O_5$ mixture with a CaO/V_2O_5 mole ratio of 1:1, the content of CaV_2O_6 steadily increased from 22% to approximately 99% as the temperature increased from 400 to 600°C.

The XRD patterns of the products of the $CaO-V_2O_5$ (2:1) mixture roasted at 400, 450, 500, 550, 600, and 650°C for 40 h revealed that the transformation of the $CaO-V_2O_5$ mixture with a mole ratio of 2:1 involves the formation of CaV_2O_6 and $Ca_2V_2O_7$. The XRD patterns of the roasted samples are

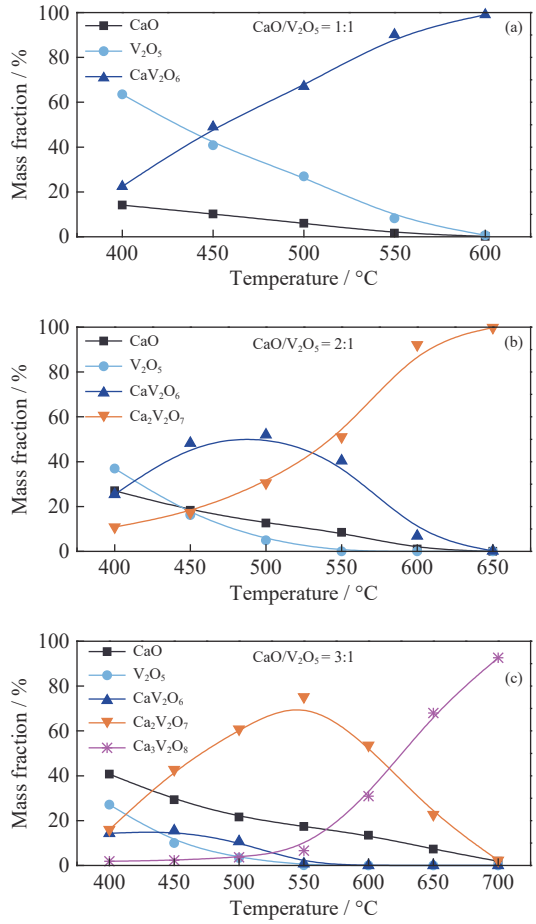

Fig. 3. Variation of the phase compositions of the $CaO-V_2O_5$ mixtures with different CaO/V_2O_5 mole ratios as a function of roasting temperature: (a) 1:1; (b) 2:1; (c) 3:1.

not shown here. As shown in Fig. 3(b), for the $CaO-V_2O_5$ mixture with a mole ratio of 2:1, the content of CaO and V_2O_5 substantially decreased with the increase in temperature and reached to zero at 650 and 550°C, respectively. However, the content of CaV_2O_6 initially increased rapidly, reached a maximum value at 500°C, and then decreased sharply at higher temperature (500–600°C), and eventually reduced close to zero at 650°C. The content of $Ca_2V_2O_7$ slightly increased at lower temperature (400–500°C), and then substantially increased at higher temperature (550–650°C) because of the solid-state reaction of CaV_2O_6 and CaO.

For the $CaO-V_2O_5$ mixture with a mole ratio of 3:1, as shown in Fig. 3(c), the main phases of the sample roasted at 400°C are CaO, V_2O_5, CaV_2O_6, and $Ca_2V_2O_7$ with a small amount of $Ca_3V_2O_8$. When the temperature increased from 400 to 550°C, the contents of CaO and V_2O_5 significantly decreased, whereas the content of CaV_2O_6 slightly increased initially and then decreased and almost disappeared at 550°C; however, the content of $Ca_2V_2O_7$ increased rapidly and reached a maximum value at 550°C. When the temperature increased from 550 to 700°C, the content of $Ca_2V_2O_7$ and

CaO substantially decreased, while the content of $Ca_3V_2O_8$ significantly increased. This indicates that the solid reaction of CaV_2O_6 and CaO is basically completed at 550°C with a final product of $Ca_2V_2O_7$, whereas the solid reaction of $Ca_2V_2O_7$ and CaO is completed at 700°C with a final product of $Ca_3V_2O_8$.

The solid-state reactions between CaO and V_2O_5 have been partly described previously [1,16,22–23]. CaV_2O_6, $Ca_2V_2O_7$, and $Ca_3V_2O_8$ may be formed by the following reactions:

$$CaO + V_2O_5 = CaV_2O_6 \quad (1)$$

$$2CaO + V_2O_5 = Ca_2V_2O_7 \quad (2)$$

$$3CaO + V_2O_5 = Ca_3V_2O_8 \quad (3)$$

$$CaO + CaV_2O_6 = Ca_2V_2O_7 \quad (4)$$

$$2CaO + CaV_2O_6 = Ca_3V_2O_8 \quad (5)$$

$$CaO + Ca_2V_2O_7 = Ca_3V_2O_8 \quad (6)$$

A plot of the standard Gibbs free energy ($\Delta G^{\ominus}$) as a function of temperature for the above reactions is shown in Fig. 4. The $\Delta G^{\ominus}$ for all the reactions is negative at low temperatures, which indicates that the above reactions are thermodynamically favorable. The values of $\Delta G^{\ominus}$ are more negative for reaction (1) than for reactions (4) and (6) below 600°C, indicating that the formation of calcium vanadate follows the order $CaV_2O_6 > Ca_2V_2O_7 > Ca_3V_2O_8$. The variation of the contents of CaV_2O_6, $Ca_2V_2O_7$, and $Ca_3V_2O_8$, presented in Fig. 3, confirm this finding.

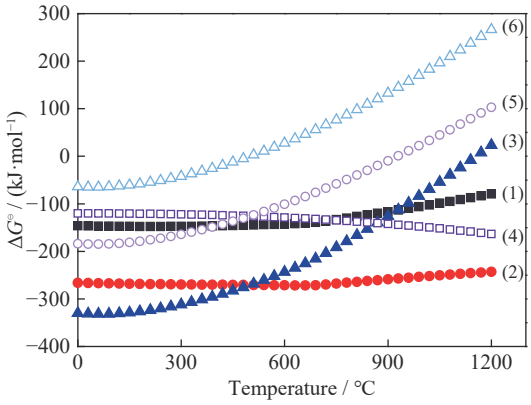

Fig. 4. $\Delta G^{\ominus}$–T plots for the possible reactions of $CaO-V_2O_5$ mixture.

3.3. Solid-state reaction kinetics

Examination of the solid-state reaction kinetics of the $CaO-V_2O_5$ system using TG–DSC is very difficult because there should be no theoretical weight change except the release of water molecules and the volatilization of V_2O_5 during the heating process (as shown in Fig. 1). Furthermore, the enthalpy changes in the solid-state reaction of $CaO-V_2O_5$ system are small and complex, and therefore difficult to distinguish from noise and the heat of the phase transformation. Therefore, the solid-state reaction kinetics of the $CaO-V_2O_5$ system was investigated by examining the phase variation of the samples roasted at different temperatures and holding times. The formation of CaV_2O_6 is the basis of the formation of other types of calcium vanadates and the most important intermediate product in the vanadium extraction process. Therefore, the solid-state reaction kinetics of the representative $CaO-V_2O_5$ (1:1) mixture was investigated. The XRD patterns of the products of the $CaO-V_2O_5$ (1:1) mixture roasted at 450, 500, and 550°C for different times are performed (figure not given here). The XRD diffraction intensity of V_2O_5 gradually decreased with the increase of roasting temperature and the extending of reaction time, whereas the XRD diffraction intensity of CaV_2O_6 gradually increased.

The preliminary quantitative phase analysis of the XRD patterns was used to determine the mass fraction of CaV_2O_6. The variation of CaV_2O_6 in the $CaO-V_2O_5$ mixture with reaction temperature and time is shown in Fig. 5. The formation rate of CaV_2O_6 substantially increased with the increase in temperature from 450 to 500°C and slightly increased with a further increase to 550°C. Furthermore, the yield of CaV_2O_6 increased almost linearly with time at 450°C, while it initially increased exponentially and then increased slightly at 500 and 550°C.

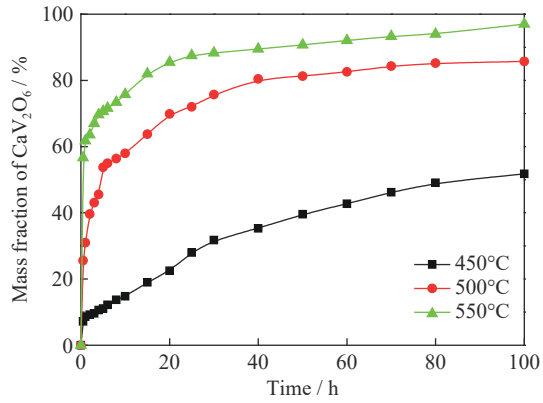

Fig. 5. Mass fraction of CaV_2O_6 in the $CaO-V_2O_5$ (1:1) mixture roasted at 450, 500, and 550°C for different times.

The heterogeneous solid-state reaction is generally expressed as [24],

$$\frac{d\alpha}{dt} = k(T)\,f(\alpha) \quad (7)$$

$$\alpha = \frac{w}{100} \quad (8)$$

where α is the degree of conversion, w is the mass percentage of product, t is the time, and T is the temperature. The reaction rate constant $k(T)$ follows the Arrhenius expression:

$$k(T) = A\exp\left(-\frac{E_a}{RT}\right) \quad (9)$$

Combining Eqs. (7) and (9) gives

$$\frac{d\alpha}{dt} = A\exp\left(-\frac{E_a}{RT}\right)f(\alpha) \quad (10)$$

In Eqs. (9) and (10), R is the gas constant and A, E_a, and $f(\alpha)$ are the so-called "kinetic triplet." A is the preexponential factor, E_a is the activation energy, and $f(\alpha)$ is a differential function that represents the reaction model. Integration of Eq. (10) leads to another integral function that represents the kinetic model:

$$g(\alpha) = \int_0^\alpha \frac{d\alpha}{f(\alpha)} = A\int_0^t \exp\left(-\frac{E_a}{RT}\right)dt \quad (11)$$

The kinetic parameters can be obtained using the model-free approach method or the model fitting method. The model-free approach method in isothermal kinetics helps to avoid the problems that originate from the ambiguous evaluation of the reaction model [25]; however, it needs continuous experimental data points. The experimental data were applied to the most commonly used kinetic reaction models such as reaction order, diffusion, nucleation, and geometrical contraction. According to the model fitting results, the second-order reaction model has the highest regression coefficients at all temperatures and can therefore be considered more suitable for describing the kinetics of the solid-state reaction of the $CaO–V_2O_5$ mixture. The straights lines shown in Fig. 6 indicate that the second-order model can well represent the solid reaction process. Thus, the equation representing the kinetics of this process can be written as

$$g(\alpha) = (1-\alpha)^{-1} - 1 = kt \quad (12)$$

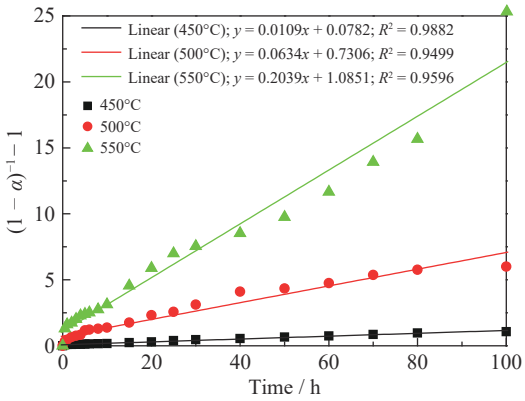

Fig. 6. Variation of $(1-\alpha)^{-1}-1$ with time for the solid reaction of the $CaO–V_2O_5$ (1:1) mixture.

The activation energy of the reaction can be determined using the Arrhenius equation. Taking the natural logarithm on both sides of Eq. (9) [26],

$$\ln k = \ln A - \frac{E_a}{RT} \quad (13)$$

When the reaction obeys the Arrhenius equation, a plot of $\ln k$ versus $1/T$ is a straight line with slope $-E_a/R$ and intercept $\ln A$. The Arrhenius plot of $\ln k$ versus $1/T$, shown in Fig. 7, gives an apparent activation energy of 145.38 kJ/mol and a preexponential factor A of 3.67×10^8 min^{-1} for the solid reaction of the $CaO–V_2O_5$ (1:1) mixture.

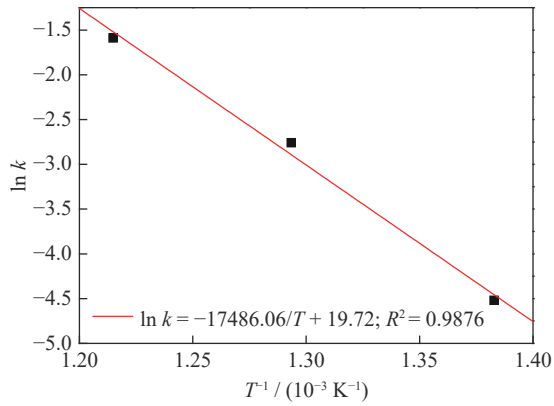

Fig. 7. Arrhenius plot for the solid reaction of the $CaO–V_2O_5$ (1:1) mixture.

3.4. SEM/EDS analysis

Fig. 8 shows the back-scattered electron (BSE) micrographs of the $CaO–V_2O_5$ (1:1) mixture roasted at 450°C for 100 h. The image shows two types of particles with different BSE intensities agglomerated together, a bright white one and a gray one. The bright white particles are approximately spherical or ellipsoidal with a diameter of 2–4 μm, whereas the gray particles are amorphous with a wide range of sizes (Figs. 8(a) and 8(b). Figs. 8(c)–8(f) show the elemental distribution maps of V, Ca, O, and C for the region marked by a white square in Fig. 8(b). Ca is obviously enriched in the gray particles, whereas V is enriched in the white particles. These results indicate that the solid-state reaction of V_2O_5 and CaO is incomplete under the roasting conditions of 450°C and 100 h.

The BSE micrographs of the $CaO–V_2O_5$ mixture roasted at 550°C for 100 h are shown in Fig. 9. No samples with significantly different gray levels are observed in Figs. 9(a) and 9(b). Compared with the samples roasted at 450°C, the morphology of the particles roasted at 550°C tends to be uniform. The particles are almost spherical and obviously sintered together (Fig. 9(b)). As shown in Figs. 9(c)–9(f), the EDS patterns show that points 1 to 4 in Fig. 9(b) all enriched with Ca, V, and O. Furthermore, the atomic proportions of Ca, V, and O are close to that of CaV_2O_6. This result means that the solid reaction of the $CaO–V_2O_5$ mixture ran to completion under the roasting conditions of 550°C and 100 h. The change in the sample morphology is basically consistent with the study on calcification roasting of vanadium slag. With an increase in temperature (660–900°C), the vanadate transforms in morphology from a small amount of dissemination to microparticles and an amorphous molten zone and migrates to the outside of the slag particles [27].

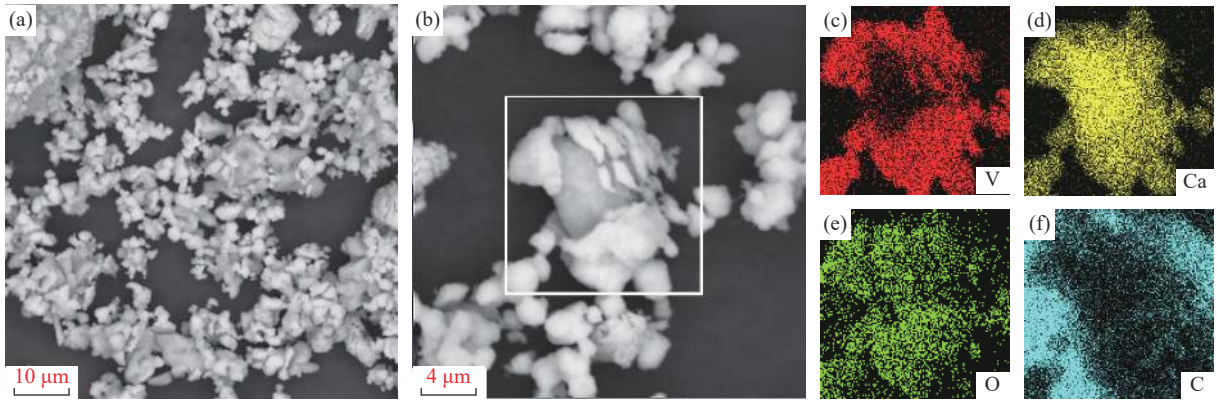

Fig. 8. (a, b) Back-scattered electron (BSE) micrographs of the $CaO-V_2O_5$ (1:1) mixture roasted at 450°C for 100 h; elemental distribution maps of the region marked by a white square in (b): (c) V; (d) Ca; (e) O; (f) C.

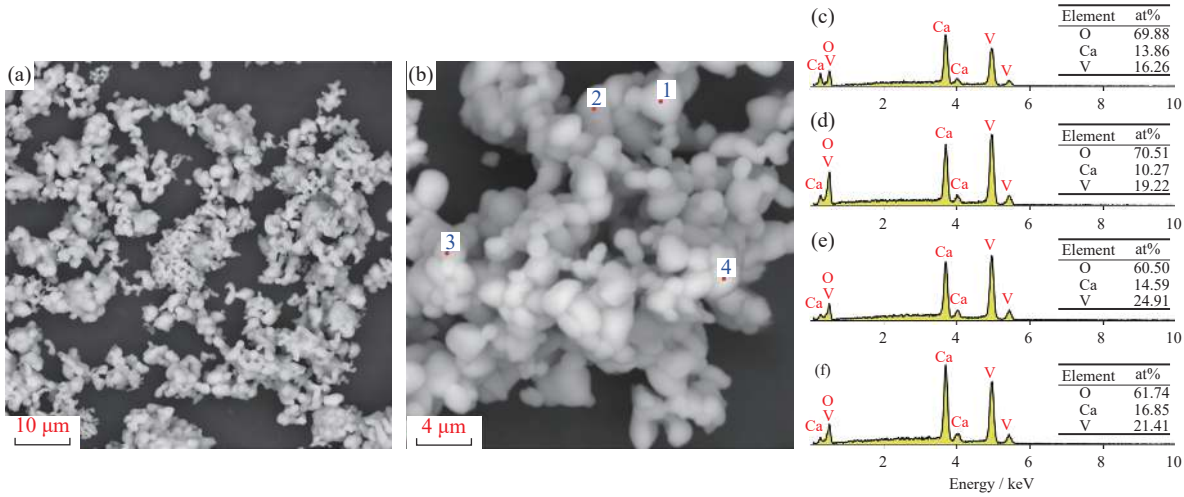

Fig. 9. (a, b) Back-scattered electron (BSE) micrographs of the $CaO-V_2O_5$ (1:1) mixture roasted at 550°C for 100 h; EDS patterns of points 1–4 in (b): (c) point 1; (d) point 2; (e) point 3; (f) point 4.

4. Conclusions

The phase transformation and solid-state reaction kinetics of a $CaO-V_2O_5$ mixture were investigated in the present study. The following conclusions can be drawn.

(1) The solid reaction of the $CaO-V_2O_5$ mixture is strongly influenced by the reaction temperature and CaO/V_2O_5 mole ratio. The transformation of calcium vanadates goes through a step-by-step solid-state reaction of $CaO-V_2O_5$. The formation of CaV_2O_6 involves the simple solid reaction of $CaO-V_2O_5$. The generation of $Ca_2V_2O_7$ involves the formation of CaV_2O_6 and the reaction of CaV_2O_6–CaO. However, the formation of $Ca_3V_2O_8$ involves the formation of CaV_2O_6 and CaV_2O_7. Only the CaV_2O_6, $Ca_2V_2O_7$, and $Ca_3V_2O_8$ phases can be detected at 600, 650, and 700°C for the solid-state reaction of the $CaO-V_2O_5$ mixture with a CaO/V_2O_5 mole ratio of 1:1, 2:1, and 3:1, respectively.

(2) The thermal analysis shows that the fusion of V_2O_5 and CaV_2O_6 occurred at 623.4 and 769.7°C, respectively. The solid reaction of the $CaO-V_2O_5$ (1:1) mixture is strongly influenced by the reaction temperature and time. The mass fraction of CaV_2O_6 linearly increased with holding time at 450°C, whereas it substantially increased initially and then remained roughly stable above 500°C. With the increase in temperature from 450 to 550°C at a reaction time of 100 h, the samples changed from parts of unreacted material with irregular shapes to the CaV_2O_6 product with an approximately uniform and spherical morphology.

(3) Graphical and statistical methods show that the reaction of $CaO-V_2O_5$ (1:1) can be described using a second-order reaction model in the form of $(1-\alpha)^{-1}-1=kt$. The E_a and A for the solid reaction of $CaO-V_2O_5$ (1:1) were determined to be 145.38 kJ/mol and 3.67×10^8 min^{-1}, respectively.

Acknowledgements

This work was financially supported by the National Natural Science Foundation of China (No. 52004044), the Natural Science Foundation of Chongqing, China (No. cstc2019jcyj-bshX0068), Chongqing Postdoctoral Innova-

tion Program (No. CQBX201904), and the Open Project Founded by the State Key Laboratory of Vanadium and Titanium Resources Comprehensive Utilization.

References

[1] J.H. Zhang, W. Zhang, L. Zhang, and S.Q. Gu, Mechanism of vanadium slag roasting with calcium oxide, *Int. J. Miner. Process.*, 138(2015), p. 20.

[2] C.K. Gupta and N. Krishnamurthy, *Extractive Metallurgy of Vanadium*, Elsevier Science Publishers B.V., Amsterdam, 1992, p. 76.

[3] R. Navarro, J. Guzman, I. Saucedo, J. Revilla, and E. Guibal, Vanadium recovery from oil fly ash by leaching, precipitation and solvent extraction processes, *Waste Manage.*, 27(2007), No. 3, p. 425.

[4] J.X Liu, L.J. Li, S.L. Zheng, S.N. Wang, H. Du, and H.Y. Xie, Extraction of vanadium from vanadium-containing slag by roasting-hydrothermal alkali leaching, *Chin. J. Process Eng.*, 14(2014), No. 5, p. 763.

[5] J.Y. Xiang, Q.Y. Huang, X.W. Lv, and C.G. Bai, Extraction of vanadium from converter slag by two-step sulfuric acid leaching process, *J. Cleaner Prod.*, 170(2018), p. 1089.

[6] Z.M. Cao, N. Wang, W. Xie, Z.Y. Qiao, and I.H. Jung, Critical evaluation and thermodynamic assessment of the $MgO-V_2O_5$ and $CaO-V_2O_5$ systems in air, *Calphad*, 56(2017), p. 72.

[7] Y. Yang, H.H. Mao, and M. Selleby, An assessment of the Ca−V−O system, *Calphad*, 56(2017), p. 29.

[8] H.Y. Li, K. Wang, W.H. Hua, Y. Zhao, W. Zhou, and B. Xie, Selective leaching of vanadium in calcification-roasted vanadium slag by ammonium carbonate, *Hydrometallurgy*, 160(2016), p. 18.

[9] Z.B. Fu, Experimental research on vanadium extraction by calcified roasting and acid leaching, *Iron Steel Vanadium Titanium*, 35(2014), No. 1, p. 1.

[10] H.S. Chen, Study on extracting vanadium pentoxide from roasted vanadium slag with lime, *Iron Steel Vanadium Titanium*, 1992, No. 6, p. 1.

[11] T.I. Krasnenko, T.P. Sirina, and M.V. Rotermel, Phase equilibria in the $V_2O_5-NaVO_3-Ca(VO_3)_2-Mn_2V_2O_7$ system and interactions of phases with H_2SO_4 and NaOH solutions, *Russ. J. Inorg. Chem.*, 53(2008), art. No. 1489.

[12] Z.H. Wang, L. Chen, T. Aldahrib, C. Li, W.Z. Liu, G.Q. Zhang, Y.H. Yang, and D.M. Luo, Direct recovery of low valence vanadium from vanadium slag—Effect of roasting on vanadium leaching, *Hydrometallurgy*, 191(2020), art. No. 105156.

[13] J. Wen, T. Jiang, J.P. Wang, H.Y. Gao, and L.G. Lu, An efficient utilization of high chromium vanadium slag: Extraction of vanadium based on manganese carbonate roasting and detoxification processing of chromium-containing tailings, *J. Hazard. Mater.*, 378(2019), art. No. 120733.

[14] M. Li, B. Liu, S.L. Zheng, S.N. Wang, H. Du, D.B. Dreisinger, and Y. Zhang, A cleaner vanadium extraction method featuring non-salt roasting and ammonium bicarbonate leaching, *J. Cleaner Prod.*, 149(2017), p. 206.

[15] T. Jiang, J. Wen, M. Zhou, and X.X. Xue, Phase evolutions, microstructure and reaction mechanism during calcification roasting of high chromium vanadium slag, *J. Alloys Compd.*, 742(2018), p. 402.

[16] G.B. Sadykhov, K.V. Goncharov, T.V. Goncharenko, and T.V. Olyunina, Phase transformations during the oxidation of calcium-containing titanium-vanadium slags and their influence on the formation of calcium vanadates, *Russ. Metall.*, 2013(2013), No. 3, p. 161.

[17] H.Y. Gao, T. Jiang, Y.Z. Xu, J. Wen, and X.X. Xue, Leaching kinetics of vanadium and chromium during sulfuric acid leaching with microwave and conventional calcification-roasted high chromium vanadium slag, *Miner. Process. Extr. Metall. Rev.*, 41(2020), No. 1, p. 22.

[18] J.Y. Xiang, Q.Y. Huang, X.W. Lv, and C.G. Bai, Effect of mechanical activation treatment on the recovery of vanadium from converter slag, *Metall. Mater. Trans. B*, 48(2017), No. 5, p. 2759.

[19] J. Wen, T. Jiang, Y.Z. Xu, J.Y. Liu, and X.X. Xue, Efficient separation and extraction of vanadium and chromium in high chromium vanadium slag by selective two-stage roasting–leaching, *Metall. Mater. Trans. B*, 49(2018), No. 3, p. 1471.

[20] L.B. Mccusker, R.B. Von Dreele, D.E. Cox, D. Louër, and P. Scardi, Rietveld refinement guidelines, *J. Appl. Crystallogr.*, 32(1999), p. 36.

[21] L. Sobrados, S. Goni, J.L. Sagrera, and M.J. Martinez, Study of the evolution of $CaCO_3-V_2O_5$ (1:1) mixture at room temperature by thermal analysis, *J. Therm. Anal.*, 38(1992), No. 4, p. 997.

[22] Y. Zhao, H.Y. Li, X.C. Yin, Z.M. Yan, X.M. Yan, and B. Xie, Leaching kinetics of calcification roasted vanadium slag with high CaO content by sulfuric acid, *Int. J. Miner. Process.*, 133(2014), p. 105.

[23] J. Wen, T. Jiang, M. Zhou, H.Y. Gao, J.Y. Liu, and X.X. Xue, Roasting and leaching behaviors of vanadium and chromium in calcification roasting–acid leaching of high-chromium vanadium slag, *Int. J. Miner. Metall. Mater.*, 25(2018), No. 5, p. 515.

[24] S. Vyazovkin, A.K. Burnham, J.M. Criado, L.A. Pérez-Maqueda, C. Popescu, and N. Sbirrazzuoli, ICTAC Kinetics Committee recommendations for performing kinetic computations on thermal analysis data, *Thermochim. Acta*, 520(2011), No. 1-2, p. 1.

[25] S. Vyazovkin and C.A. Wight, Isothermal and non-isothermal kinetics of thermally stimulated reactions of solids, *Int. Rev. Phys. Chem.*, 17(1998), No. 3, p. 407.

[26] H.M. Liu, M.Q. Chen, Z.L. Han, and B.A. Fu, Isothermal kinetics based on two-periods scheme for co-drying of biomass and lignite, *Thermochim. Acta*, 573(2013), p. 25.

[27] N.X. Fu, L. Zhang, W.H. Liu, B. Zhao, G.F. Tu, and Z.T. Sui, Mechanism analysis of phase transformation process in calcified roasting of vanadium slags, *Chin. J. Nonferrous Met.*, 28(2018), No. 2, p. 377.